

Temperature evolution of self-organized stripe domains in ultrathin Fe films on MnAs/GaAs(001)C. Helman,^{1,2} J. Milano,^{2,3,4,*} S. Tacchi,⁵ M. Madami,⁵ G. Carlotti,^{5,6} G. Gubbiotti,⁵ G. Alejandro,^{2,3} M. Marangolo,^{2,4} D. Demaille,^{2,4} V. H. Etgens,^{2,4} and M. G. Pini⁷¹*CNEA, Centro Atómico Constituyentes, Avenida General Paz 1499, San Martín, Argentina*²*Laboratorio Internacional Franco-Argentino en Nanociencias (LIFAN)*³*CNEA, Centro Atómico Bariloche, San Carlos de Bariloche, R8402AGP Río Negro, Argentina*⁴*INSP, UPMC Paris 06, CNRS UMR 7588, 140 Rue de Lourmel, 75015 Paris, France*⁵*CNISM, Dipartimento di Fisica, Università di Perugia, Via A. Pascoli, I-06123 Perugia, Italy*⁶*Centro S3, CNR-Istituto di Nanoscienze, Via Campi 213A, I-41125 Modena, Italy*⁷*Istituto dei Sistemi Complessi, CNR, Via Madonna del Piano 10, Sesto Fiorentino, I-50019 Firenze, Italy*

(Received 11 June 2010; published 14 September 2010)

A detailed investigation of the magnetic behavior of an ultrathin Fe film epitaxially grown onto MnAs/GaAs(001) is performed by means of both ferromagnetic resonance (FMR) and magneto-optical Kerr-effect (MOKE) experiments, as a function of temperature. When the MnAs underlayer is fully in the hexagonal ferromagnetic α phase (at low temperature) or in the orthorhombic non magnetic β one (at high temperature), the magnetic behavior of the Fe film is found to be nearly the same and independent of the substrate. In contrast, at intermediate temperatures, when the MnAs underlayer presents a self-organized phase consisting of α -MnAs and β -MnAs striped domains, the Fe film is strongly influenced by the dipolar (stray) fields arising from the substrate. As a consequence, the Fe film breaks in two distinct families of striped domains. Theoretical analysis of the FMR data in the whole investigated temperature range is performed using a free-energy density model which provides an accurate determination of the temperature-dependent magnetic parameters. Furthermore, the mechanism of magnetization reversal has been analyzed as a function of temperature by MOKE. The evolution of the magnetization curves can be satisfactorily interpreted starting from the main achievements of the theoretical analysis of FMR data.

DOI: [10.1103/PhysRevB.82.094423](https://doi.org/10.1103/PhysRevB.82.094423)

PACS number(s): 76.50.+g, 78.20.Ls, 75.60.-d, 75.70.-i

I. INTRODUCTION

The search for spatially self-organized nanostructures has received strong impetus owing to their potential use as storage media in magnetoelectronic devices,¹ as well as due to their relatively straightforward growth. In this context, MnAs/GaAs(001) thin films show an interesting self-organization phenomenon, induced by a temperature change around room temperature, that involves both structural and magnetic transformations.² In fact, the difference between the thermoelastic coefficients of MnAs and GaAs induces a strain in the MnAs layer. Therefore, in the neighborhood of the magnetostructural transition ($T_C=313$ K) of bulk MnAs,³ the elastic energy of the MnAs film is minimized through self-organization in a regular array of stripes that alternate two component phases. The two phases are found to coexist in a temperature range of about 40 K around room temperature. They differ in both the structural and the magnetic properties: the low-temperature α phase is hexagonal and ferromagnetic while the high-temperature β phase is orthorhombic and nonmagnetic. The two phases display different heights at the film surface, as it is sketched in Fig. 1(a): the α phase corresponds to ridges, the β phase to grooves. The period p and height h of the stripes are determined by the MnAs thickness t : $p \approx 4.8t$ and $h \approx 0.01t$. For a given thickness, the sample temperature determines the relative width of α and β stripes within the coexistence region.^{2,4-10} Furthermore, MnAs/GaAs(001) as a magnetic template presents interesting properties for being used in devices with external control capabilities, both in order to en-

code information (writing process) and to recover data (reading process). In Ref. 11, an MnAs/GaAs(001) film was used as a template for growing an ultrathin Fe film. With respect to the direction of the substrate magnetization, the Fe magnetization was found to switch from parallel to antiparallel, and back to parallel, upon increasing the sample temperature from 293 to 313 K (a temperature range comprised within the coexistence region of the α and β phases of MnAs). The effect was successfully explained¹¹ by considering the stray field generated by the finite size of the α -MnAs stripes [see Fig. 1(a)]: the α -MnAs magnetization is substantially within the film plane and perpendicular to the stripes so that, at the border between two stripes, “magnetic poles” are created. This means that the switching of the Fe magnetization is driven by effective magnetic fields arising from the temperature-dependent magnetic structure of the self-organized MnAs/GaAs(001) template. A straightforward application of the temperature control of the Fe magnetization without applying any magnetic field was reported in Ref. 12 where the idea of a magnetically active template was introduced.

More recently, some of us exploited Brillouin light scattering (BLS) to perform a quantitative analysis of the spin-wave frequencies in Fe/MnAs/GaAs(001).¹³ This allowed us to achieve a quantitative estimate of the stray fields produced by the α -MnAs stripes at two different sample temperatures. During the coexistence of the MnAs stripes, it was found that the Fe/MnAs/GaAs(001) system behaves as an array of alternated Fe/ α -MnAs and Fe/ β -MnAs stripes. We argued¹³ that a domain-wall structure at the Fe stripe edges isolates, both statically and dynamically, adjacent Fe stripe domains

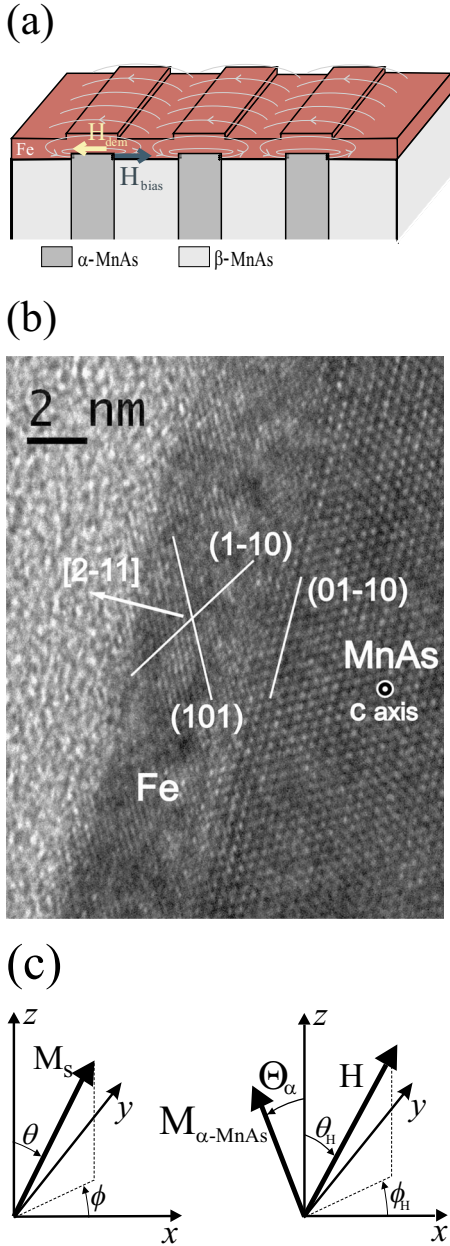


FIG. 1. (Color online) (a) Schematic view of the investigated system, a 4-nm-thick Fe film epitaxially grown on MnAs/GaAs(001). The magnetic force lines in the Fe overlayer, according to the stray field model, are also displayed. (b) TEM image of Al-capped Fe/MnAs/GaAs(001) taken along [0001] zone axis (*c* axis) of MnAs. (c) Reference frames for the magnetization of Fe (left) and that of α -MnAs (right).

in a manner analogous to a “lateral” exchange spring.

Moreover, a preliminary study of the system was performed by using ferromagnetic resonance (FMR) experiments in the temperature range where the α and β phases of MnAs coexist.¹⁴ The resonance field, linewidth, and shape of the Fe line were found to be strongly altered, and a non-monotonic temperature behavior of the Fe resonance field was observed in a few kelvin range.¹⁴

In this work, we present a systematic study of the magnetic properties of the Fe/MnAs/GaAs(001) system in a wide

range of temperatures by using two complementary techniques: FMR and magneto-optic Kerr effect (MOKE). From a quantitative analysis of the FMR experimental results, we extracted the temperature dependence of the magnetic anisotropies of the Fe layer, as well as of the stray fields produced on the Fe overlayer by the MnAs/GaAs(001) template in the striped phase. The MOKE technique was then exploited to study the influence of the magnetostatical properties of the MnAs substrate on the magnetization reversal process of the Fe film.

The paper is organized as follows. In Sec. II, details about sample preparation and experimental techniques are provided. Sections III–V are devoted to the presentation of experimental data and the discussion of results. Finally, the conclusions are drawn in Sec. VI.

II. EXPERIMENTAL

The sample was prepared by molecular beam epitaxy (MBE). After oxide desorption under As flux, a thick GaAs buffer layer was grown on the GaAs(001) substrate at 833 K in As-rich conditions. The sample temperature was then reduced to 503 K. The growth of the 140-nm-thick MnAs film followed the procedure described by Tanaka *et al.*¹⁵ to obtain an MnAs film with A orientation, as it was confirmed *in situ* by reflection high-energy electron diffraction (RHEED) analysis and *ex situ* by x-ray diffraction. Keeping the ultra-high vacuum, the sample was moved to another chamber and a 4-nm-thick Fe layer was deposited by using a Knudsen cell on the MnAs substrate kept at 423 K, a temperature where MnAs is single phased (γ phase) and does not display any stripe pattern. A half of the same MnAs substrate was not exposed to the Fe evaporation to serve as a reference sample. *In situ* RHEED and *ex situ* transmission electron microscopy (TEM) analysis showed that Fe epitaxially grows on MnAs, with $(2\bar{1}1)_{\text{Fe}} \parallel (1\bar{1}00)_{\text{MnAs}} \parallel (001)_{\text{GaAs}}$ and $[11\bar{1}]_{\text{Fe}} \parallel [0001]_{\text{MnAs}} \parallel [1\bar{1}0]_{\text{GaAs}}$, as shown in Fig. 1(b). Finally, the Fe layer was capped by 2 nm of Al for protection during the transportation in air.

The FMR measurements were performed in an ESP-300 Bruker spectrometer operating at a microwave frequency of 9.45 GHz (X band). Measurements with the static magnetic field H rotating in the plane of the samples [varying the angle ϕ_H in Fig. 1(c)] were done, with the aim of characterizing the Fe magnetic anisotropy and the effective magnetic coupling between Fe and MnAs. Detailed temperature-dependent measurements were performed, in the temperature range between 240 and 340 K. Hysteresis loops have been measured with a conventional MOKE apparatus based on a photoelastic modulator, working in longitudinal configuration (i.e., with the external field parallel to the sample surface and to the plane of incidence of light). In this configuration, the signal collected from a photodiode is proportional to the in-plane component of the magnetization parallel to the applied field. Measurements as a function of the temperature have been performed placing the sample inside a cryostat whose temperature can be set in the range (100–500) K. For each temperature, we measured two hysteresis curves changing the position of the focused light spot on the sample. In

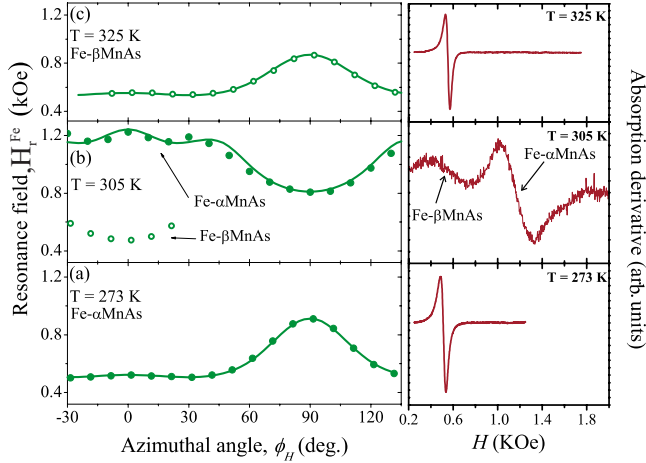


FIG. 2. (Color online) Left panel: resonance field, H_r^{Fe} , of Fe versus ϕ_H , azimuthal angle of the in-plane applied field, for three different sample temperatures. The lines through the experimental points are the simulation results. (a) $T=273$ K (pure α -MnAs phase); (b) $T=305$ K (striped phase, the arrows indicate the two Fe resonance modes); (c) $T=325$ K (pure β -MnAs phase). Right panel: FMR spectra, taken at fixed angle $\phi_H=0^\circ$, at the same temperatures.

the first position, we measured the bare MnAs substrate while in the second one, we measured the complete Fe/MnAs heterostructure.

III. FMR STUDY

In Fig. 2, we show three typical FMR spectra as well as the resonance field of the Fe layer, H_r^{Fe} , as a function of the azimuthal angle, ϕ_H , defined in Fig. 1(c). The measurements have been performed applying the magnetic field in the sample plane ($\theta_H=90^\circ$). The data refer to three sample temperatures corresponding to different magnetostructural states of the MnAs/GaAs(001) template.

One immediately observes that both the angular dependence of the resonance field and the shape of the FMR spectrum display a quite similar behavior at low [Fig. 2(a)] and high [Fig. 2(c)] temperature, when the MnAs substrate is fully in the α phase and in the β phase, respectively. The maximum in the angular dependence of H_r^{Fe} , observed at $\phi_H=90^\circ$, signals that the $[11\bar{1}]_{\text{Fe}}$ crystallographic direction is a hard magnetic axis for the Fe film, both for low ($T=273$ K) and for high temperatures ($T=325$ K).¹⁶ At an intermediate temperature ($T=305$ K), characterized by the coexistence of α -MnAs and β -MnAs stripes in the substrate, the FMR response of the Fe overlayer totally changes [Fig. 2(b)]. In fact, the Fe signal becomes more noisy and a second broad and weak Fe mode appears in the FMR spectra, taken applying the magnetic field in a range of angles around $\phi_H=0^\circ$. Remarkably, if one looks at the behavior of the most intense peak, the $[11\bar{1}]_{\text{Fe}}$ crystallographic direction along which the stripe pattern is aligned [the y axis in Fig. 1(c)] becomes an easy magnetization direction for Fe: in fact, a minimum is now observed at $\phi_H=90^\circ$ in the angular dependence of H_r^{Fe} .

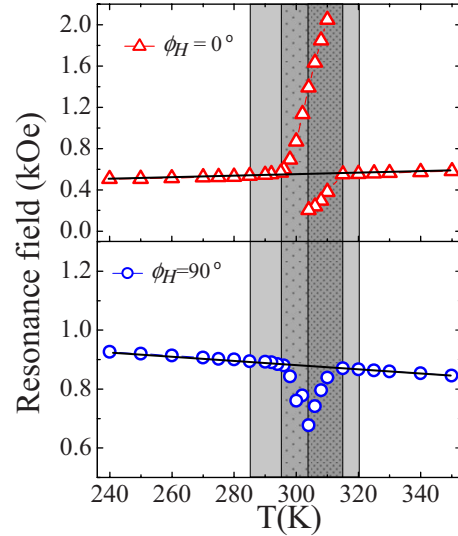


FIG. 3. (Color online) Fe resonance field, H_r^{Fe} , versus temperature, for magnetic field applied within the film plane along (hollow blue circles, $\phi_H=90^\circ$) and perpendicular to the stripes direction (hollow red triangles, $\phi_H=0^\circ$). The black lines are guide to the eyes. It is apparent that, outside the coexistence region (gray-shaded area), H_r^{Fe} presents the same linear behavior, for a fixed field orientation. The sparse and dense dotted areas correspond to the temperature ranges where there is an appreciable influence of the dipolar fields, due to the stripe formation, on the measured frequencies. In the dense dotted area, two distinct peaks are detected for $\phi_H=0^\circ$.

In Fig. 3, H_r^{Fe} is plotted versus temperature, for the magnetic field applied either perpendicular ($\phi_H=0^\circ$, triangles) or parallel to the stripes ($\phi_H=90^\circ$, circles). Between about 240 and 285 K, when the MnAs substrate is fully in the α phase, H_r^{Fe} presents a monotonous, linear dependence on temperature for both the measured H directions. For the field applied along the x direction ($\phi_H=0^\circ$), the slope is small and positive while it is small and negative for the field applied along the y direction ($\phi_H=90^\circ$). The same linear trend is also observed for temperatures higher than about 320 K, when the MnAs template is fully in the β phase. The black lines through the points in Fig. 3 clearly show that the resonance fields have the same monotonous temperature behavior both before and after the coexistence region.

Within the coexistence of the α and β phases in the MnAs template (for T between about 285 and 320 K, gray-shaded areas in Fig. 3), H_r^{Fe} shows a more complicated temperature behavior. At the initial stage of the MnAs transition, for T between 285 and 293 K, the resonance field H_r^{Fe} continues to follow the linear trend for both the field orientations. Upon increasing the sample temperature, for T between 295 and 315 K (dotted areas in Fig. 3), the behavior of H_r^{Fe} dramatically changes. When H is applied at $\phi_H=0^\circ$ (upper panel in Fig. 3), H_r^{Fe} starts to increase very rapidly with temperature, reaching a value of about 2.1 kOe for $T=310$ K.¹⁷ At a temperature of 304 K, a second Fe mode appears in the spectra (dense dotted area). The resonance field of this peak starts from a value of about 0.2 kOe at $T=304$ K and increases with temperature up to recover the linear trend (with a small, positive slope).

When H is applied at $\phi_H=90^\circ$ (lower panel in Fig. 3), instead, we always observe only a single Fe mode. In the temperature range between 295 and 304 K (sparse dotted area), H_r^{Fe} rapidly decreases, up to attain a minimum of nearly 0.7 kOe at 304 K. For temperatures higher than 304 K (when two Fe modes appear in the case $\phi_H=0^\circ$), H_r^{Fe} starts increasing (dense dotted area) up to recover the linear trend.

Lastly, at the final stage of the MnAs transition (for T between 315 and 320 K), H_r^{Fe} follows, for both the field orientations, the linear trends observed outside the region of the stripe coexistence.

In the next two sections, we present a quantitative interpretation of the above-discussed experimental data.

A. Uncoupled region

We start by modeling the Fe behavior outside the temperature range where the MnAs stripes appear (uncoupled region, white areas in Fig. 3). In this case, the Fe behavior is substantially independent of the structural and magnetic state of the substrate, as it is put in evidence by the black lines in Fig. 3. In order to determine the magnetic parameters of the Fe layer from the experimental data, one can proceed as usual by considering the free-energy density of an ultrathin epitaxial Fe(2, -1, 1) film,¹⁸

$$\begin{aligned}
 F = \frac{1}{2}M_s \left\{ \left[(4\pi M_s) - \left(\frac{2K_\perp}{M_s} \right) \right] \cos^2 \theta - \left(\frac{2K_\parallel}{M_s} \right) \sin^2 \theta \cos^2 \phi \right. \\
 + \frac{1}{12} \left(\frac{2K_1}{M_s} \right) [3 \cos^4 \theta - 4\sqrt{2} \cos^3 \theta \sin \phi \sin \theta \\
 + 6 \cos^2 \theta \sin^2 \theta \cos^2 \phi \\
 + 12\sqrt{2} \cos \theta \sin \phi \sin^3 \theta \cos^2 \phi + \sin^4 \theta (4 \sin^4 \phi \\
 + 3 \cos^4 \phi)] \left. \right\} - M_s H [\cos \theta \cos \theta_H + \sin \theta \sin \theta_H \cos(\phi \\
 - \phi_H)], \quad (1)
 \end{aligned}$$

where M_s is the saturation value of the Fe magnetization vector, \mathbf{M} , while θ and ϕ are the angles that \mathbf{M} forms with the z and x axes, respectively [Fig. 1(c), left]. In Eq. (1), the first term $H_{\text{dip}}=4\pi M_s$ is the shape anisotropy field corresponding to a thin film while the second one, $H_\perp=2K_\perp/M_s$, is the interface anisotropy field arising from the broken translational symmetry along the film normal, z .

Such effective magnetic fields are competitive since they attempt to orient the magnetization parallel ($\theta=90^\circ$) and perpendicular ($\theta=0^\circ$) to the film plane, respectively. However, our measurements indicate that \mathbf{M} lies in the xy plane.

The magnetocrystalline anisotropy field $H_K=2K_1/M_s$, instead, tends to align the Fe magnetization in plane along $\phi = \pm 41^\circ$. Eventually, the in-plane uniaxial anisotropy field, $H_\parallel=2K_\parallel/M_s$, favors the $[011]_{\text{Fe}}$ in-plane direction ($\phi=0^\circ$), which is perpendicular to the direction along which the MnAs stripes develop. It has been found in previous works that this uniaxial anisotropy is induced in the Fe film by the morphology of the MnAs substrate.¹¹

The last term in Eq. (1) is the Zeeman interaction of \mathbf{M} with an external magnetic field \mathbf{H} , applied at angles θ_H and

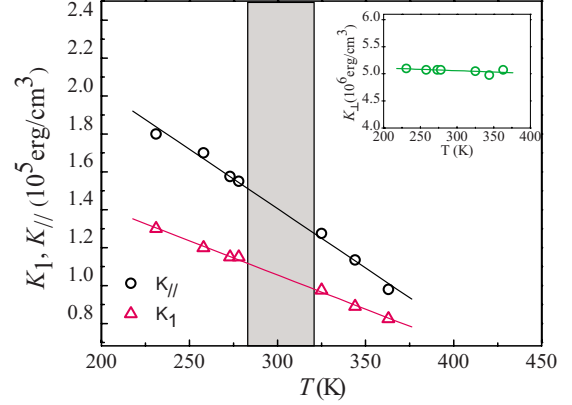


FIG. 4. (Color online) Temperature dependence of magnetocrystalline (K_1) and in-plane uniaxial (K_\parallel) anisotropy constants. Inset: temperature dependence of the uniaxial out-of-plane anisotropy K_\perp . All the plotted lines are obtained by a linear regression procedure on the relative set of data points. The shadowed area correspond to the temperature interval where coexistence of α -MnAs and β -MnAs occurs.

ϕ_H with the z and x axes, respectively [Fig. 1(c), right].

The resonance frequency, ω_r , of a ferromagnetic system is provided in terms of the second derivatives of its free-energy density by the Smit-Beljers equation,¹⁹

$$\left(\frac{\omega_r}{\gamma} \right)^2 = \frac{1}{M_s^2 \sin^2 \theta} [F_{\theta\theta} F_{\phi\phi} - (F_{\theta\phi})^2], \quad (2)$$

where γ is the gyromagnetic ratio ($\gamma=2.1$ GHz/kOe for Fe), and $F_{\theta\theta}=\frac{\partial^2 F}{\partial \theta^2}$, $F_{\phi\phi}=\frac{\partial^2 F}{\partial \phi^2}$, $F_{\theta\phi}=\frac{\partial^2 F}{\partial \theta \partial \phi}$.

In order to calculate the resonance field, H_r^{Fe} , versus the azimuthal angle, ϕ_H , the expression (2) must be evaluated at the equilibrium positions of Fe magnetization vector, determined by minimizing the energy density F . H_r^{Fe} is obtained by applying a self-consistent scheme to solve the nontrivial system obtained from Eqs. (1) and (2). Using the mentioned procedure to calculate the resonance field, the experimental data in Fig. 3 were fitted in the temperature regions outside the interval of coexistence of the α and β phases. The temperature evolution of the magnetic anisotropy constants obtained by this analysis is displayed in Fig. 4.

It appears that the magnetocrystalline (K_1) and the in-plane uniaxial (K_\parallel) anisotropy constants are of comparable strength, as expected in an ultrathin magnetic film,^{20,21} and present a linear decrease with increasing temperature in the whole investigated range, independently of the state of the underlying MnAs phase. This is similar to the temperature evolution of the uniaxial anisotropy of an Au-capped, 3-ML-thick Fe film on GaAs substrate.²² For bulk systems of localized spins, theoretical calculations predict a power-law decrease in the anisotropy constants with increasing temperature.²³ However, for ultrathin films, owing to their reduced dimensionality, the temperature dependence of the magnetization is known to be different with respect to bulk samples,^{20,21} thus the open question exists if such a power law still holds.

In our system, the magnetocrystalline anisotropy constant is found to assume values ($K_1 \sim 1 \times 10^5$ erg/cm³) nearly five times smaller than the cubic anisotropy of bulk Fe ($K_1^{\text{bulk}} = 4.8 \times 10^5$ erg/cm³).²⁴ On the other hand, the out-of-plane anisotropy parameter presents a nearly constant value, $K_{\perp} \sim 5 \times 10^6$ erg/cm³, for the whole temperature range (see inset of Fig. 4). It is worth observing that similar values for the in-plane and out-of-plane anisotropy were found²⁵ in the previous study performed by BLS technique.¹³

B. Coupled region

The analysis of the FMR results for T in the range between 295 and 315 K (coupled region) has been performed by adding to the model an effective magnetic coupling between the Fe film and the MnAs substrate, due to the stray fields produced by the latter. As shown in a previous work,¹³ the α -MnAs stripes generate two stray fields: a bias field, H_{bias} , which acts on the Fe regions put on top of the β -MnAs stripes and tends to align the Fe magnetization parallel to that of α -MnAs stripes, and a demagnetizing field, H_{dem} , which acts on the Fe regions on top of the α -MnAs stripes and tends to align the Fe magnetization antiparallel to that of α -MnAs stripes [Fig. 1(a)]. Note that in our FMR measurements only the x component of such stray fields are effective on the Fe layer. In fact, since the saturation of MnAs magnetization along the stripes axis (y) occurs for fields (≈ 30 kOe) (Ref. 26) much higher than those used in the FMR experiments, the MnAs magnetization is always confined in the vertical plane (xz).

From the temperature dependence of H_r^{Fe} (Fig. 3), one can deduce that the upper mode observed for $\phi = 0^\circ$, corresponds to Fe/ α -MnAs domains, while the lower mode to Fe/ β -MnAs ones. Thus, in the coupled region, the following expression was assumed for the free-energy density of the two-phase system:

$$F^c(T) = F(\theta_1, \phi_1, T) - M_s H_{\text{bias}}^x \sin \theta_1 \cos \phi_1 + F(\theta_2, \phi_2, T) - M_s H_{\text{dem}}^x \sin \theta_2 \cos \phi_2, \quad (3)$$

where $F(\theta_i, \phi_i, T)$ is the free-energy density, given by Eq. (1), of a given type of Fe domains ($i=1$ refers to Fe/ β -MnAs and $i=2$ to Fe/ α -MnAs) in the absence of coupling with the MnAs substrate; H_{bias}^x and H_{dem}^x denote, respectively, the x components of the stray fields [Fig. 1(a)].

It should be noted that no direct exchange interaction between the magnetization of Fe/ α -MnAs and that of Fe/ β -MnAs was assumed in Eq. (3). Such an approximation is supported by recent BLS measurements in the same system,¹³ suggesting that a domain-wall structure at the Fe stripe edges isolates (both statically and dynamically) adjacent Fe stripe domains in a way analogous to a lateral exchange spring. The shape anisotropy of the Fe stripes was also neglected.²⁷

Considering that in our FMR experiment, the Fe magnetization is always parallel to the direction of the applied field, ($\phi_i \approx \phi_H$), the spin-wave frequency of a Fe stripe, $\omega_{r,i}^{\text{Fe}}$, obtained from the Smit-Beljers Eq. (2), can be expressed as

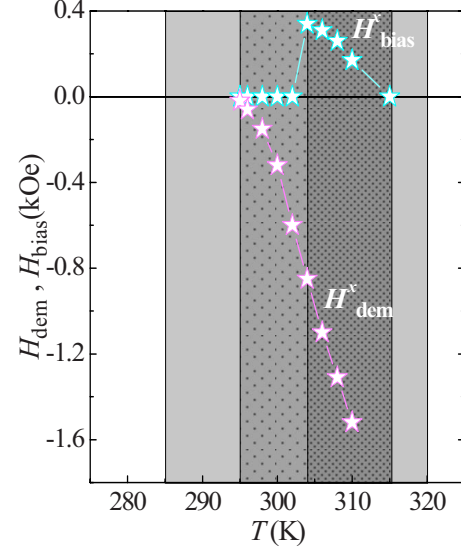


FIG. 5. (Color online) Temperature dependence of the stray fields produced, in the striped phase, by the magnetization of the MnAs/GaAs(001) template on the ultrathin Fe overlayer. H_{dem} is the stray field acting on Fe/ α -MnAs, and H_{bias} is the stray field acting on Fe/ β -MnAs.

$$\left(\frac{\omega_{r,i}^{\text{Fe}}}{\gamma} \right)^2 = \left\{ H_{r,i}^{\text{Fe}} + (4\pi M_s - H_{\perp}) + H_{\parallel} \cos^2 \phi_i + H_{\text{sf},i}^x \cos \phi_i + \frac{1}{6} H_K (11 \cos^2 \phi_i - 7 \cos^4 \phi_i - 4) \right\} \times \left\{ H_{r,i}^{\text{Fe}} + H_{\parallel} \cos(2\phi_i) + H_{\text{sf},i}^x \cos \phi_i + \frac{1}{6} H_K (29 \cos^2 \phi_i - 28 \cos^4 \phi_i - 4) \right\} - \frac{1}{2} H_K^2 (9 \cos^6 \phi_i - 12 \cos^4 \phi_i + 4 \cos^2 \phi_i), \quad (4)$$

where $H_{\text{sf},1}^x = H_{\text{bias}}^x$ and $H_{\text{sf},2}^x = H_{\text{dem}}^x$ (i.e., $i=1$ refers to Fe/ β -MnAs, and $i=2$ to Fe/ α -MnAs). The temperature dependence of the stray fields was numerically obtained from Eq. (4) by using the anisotropy parameters taken outside the striped region (Fig. 5). A detailed discussion of their evolution will be given in Sec. V.

IV. MOKE STUDY

A complementary investigation of the behavior of the Fe layer was achieved by measuring the magnetization curves in the temperature range between 255 and 326 K, using the MOKE technique. For the sake of comparison, in addition to the Fe/MnAs/GaAs(001) system, we also measured the bare MnAs/GaAs(001) template, with the same thickness of the MnAs layer.

In Fig. 6, a selection of the hysteresis loops, obtained by applying an in-plane field H in the x direction (i.e., perpendicular to the $[0001]_{\text{MnAs}}$ axis, along which the MnAs stripes develop), is reported for both the MnAs/GaAs(001) template (full dots) and the Fe/MnAs/GaAs(001) system (open dots).

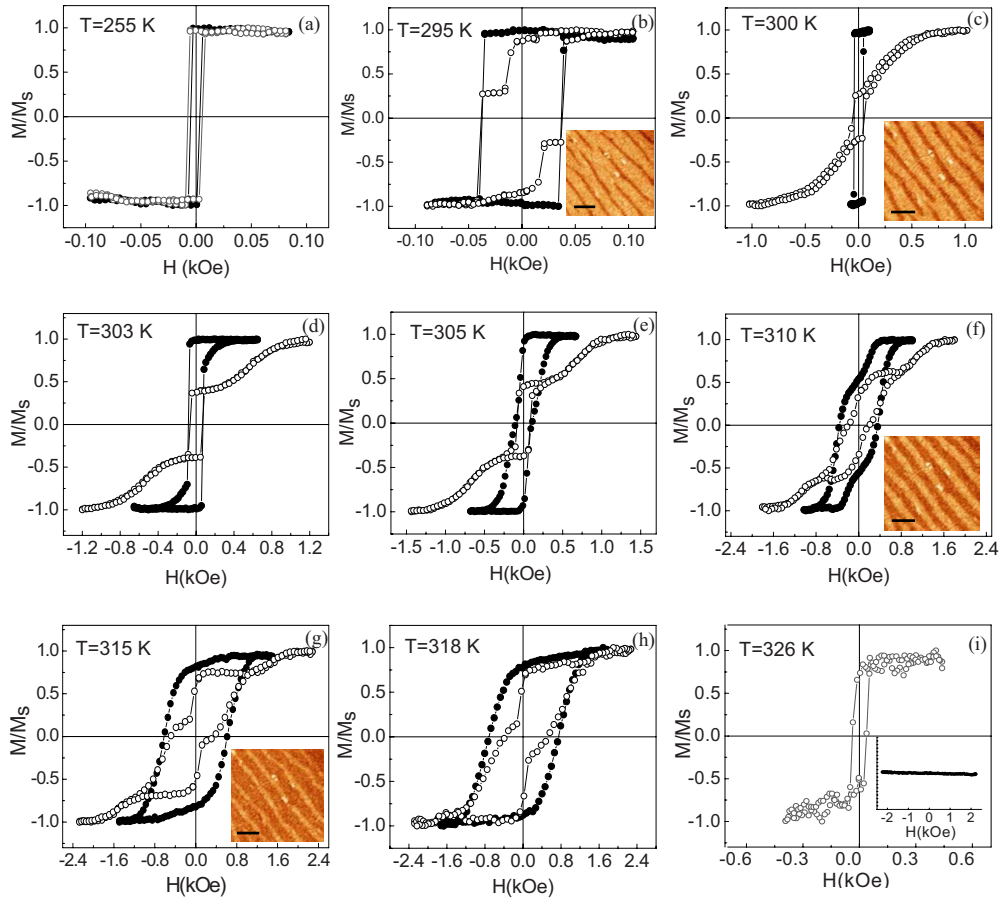


FIG. 6. (Color online) MOKE loops of the MnAs/GaAs(001) template (full symbols) and of the Fe/MnAs/GaAs(001) system (open symbols), measured at different sample temperatures T . The external magnetic field H was applied in plane along the x direction (i.e., perpendicular to the $[0001]_{\text{MnAs}}$ axis along which the MnAs stripes develop). Insets of figures: STM images of the 140-nm-thick MnAs/GaAs(001) template, obtained in constant current mode. Light-orange regions correspond to α -MnAs and dark-orange ones to β -MnAs. The scale bar represents 1 μm .

Let us first comment the evolution of the hysteresis cycles relative to the bare MnAs/GaAs layer. For sample temperature T lower than about 285 K, when the MnAs template is fully in the ferromagnetic α phase, it exhibits a well squared loop with high remanence and small coercive fields (a few oersted), a behavior typical of an easy direction [Fig. 6(a)].

In the temperature range between about 285 and 305 K, when the nonmagnetic β stripes start to appear, the cycles retain a squared shape but their coercive field increases from ≈ 20 to ≈ 70 Oe, suggesting that the nucleation of β stripes makes the reversal of magnetization more difficult [Figs. 6(b)–6(e)].²⁶

On increasing T above 305 K, instead, the hysteresis cycles of MnAs/GaAs(001) exhibit a complicated shape, characterized by a reduced value of the remanent magnetization, and by a further rapid increase in the coercive field, which attains a value of about 600 Oe at $T=315$ K [Figs. 6(f) and 6(g)]. Such a behavior, similar to that observed in previous works,²⁸ is related to the formation of a complex multidomain structure during the reversal of the MnAs magnetization. In fact, when the aspect ratio r (i.e., the ratio between the width and the thickness) of an α -MnAs stripe becomes smaller than a critical value (≈ 3), one finds that a multidomain configuration is energetically favored with re-

spect to an in-plane monodomain one. This complex configuration, which has been also studied in previous works, suggests that both in-plane and out-of-plane domains are involved.²⁸ Eventually, when the temperature approaches the transition to the fully β phase (above 318 K), there is no room for a multidomain structure anymore and the loop shape comes back to be rather squared [Fig. 6(h)].

The above discussed complex magnetization reversal process of MnAs/GaAs(001) reflects itself also on the hysteresis loops relative to the whole Fe/MnAs/GaAs(001) system, as detailed in the following. At low temperature ($T < 285$ K, when the MnAs template is fully in the α ferromagnetic phase, the Fe/MnAs/GaAs(001) system shows a squared hysteresis cycle, indistinguishable from that of the MnAs substrate.

At the onset of the MnAs transition ($T=285$ – 295 K), a double step is seen in the hysteresis loop since the coercive field of Fe is significantly lower than that of MnAs. This indicates that the magnetization reversal of the Fe layer remains almost unchanged by the MnAs transition, and Fe/MnAs/GaAs behaves as a two-phase system, with independent switching fields along the easy magnetic direction [Fig. 6(b)].

On increasing the sample temperature between 300 and 308 K, the cycles can still be seen as the superposition of the MnAs and the Fe ones but the Fe behavior changes dramatically. The horizontal plateau widens, following the coercive-field increase in MnAs, while the transition associated with the Fe film becomes smoother and smoother, indicating a coherent rotation of its magnetization [Figs. 6(c)–6(e)].

Eventually, for sample temperature higher than about 308 K, the Fe/MnAs/GaAs(001) hysteresis loops undergo a further evolution [Figs. 6(f)–6(h)]. In addition to the irreversible transition related to the MnAs substrate, one can recognize two transitions associated with the Fe layer: a reversible rotation and an abrupt jump of the magnetization around 0 Oe. In light of the above presented FMR results, the reversible rotation can be ascribed to the Fe regions put on top of α -MnAs stripes while the abrupt jump is due to the Fe regions put on top of β -MnAs stripes. Finally, when the MnAs transition to the non magnetic phase is accomplished, the Fe/MnAs/GaAs(001) system shows a squared loop typical of an easy direction [Fig. 6(i)] while no magnetic signal is detected any more from the MnAs/GaAs(001) substrate [inset of Fig. 6(i)].

V. DISCUSSION

The temperature evolution of the stray fields shown in Fig. 5, obtained by the quantitative analysis of the FMR measurements, together with the discussed evolution of the hysteresis cycles measured by MOKE, allow us to explain in detail the Fe properties in the temperature region of coexistence of the α and β phases.

At the onset of the MnAs transition ($T < 295$ K, when the β phase starts to appear but the striped pattern is not well outlined, the stray fields produced by the α -MnAs stripes are very feeble. As a consequence, the Fe layer is unaffected by the MnAs phase transition and behaves as a continuous film, with the easy magnetic axis perpendicular to the direction of the stripes. In the temperature range between 295 and 302 K, when the striped pattern becomes better defined but the α -MnAs phase is still predominant, the Fe layer continues to behave as a uniform film but its magnetic properties dramatically change, i.e., $|H_{\text{dem}}^x|$ grows significantly (Fig. 5). As a consequence, when the field is applied along this direction, the resonance field H_r^{Fe} increases monotonously with temperature (Fig. 3 upper panel). In agreement with this observation, also the magnetization reversal proceeds through a coherent rotation, which leads to antiparallel alignment between the magnetization of the Fe overlayer and that of the MnAs substrate. In this temperature region, the domain-wall structure at the Fe stripe edges is not effective in order to magnetically isolate the two kinds of domains; then the behavior of the Fe film is driven by the Fe/ α -MnAs domains, which are wider than the Fe/ β -MnAs ones.

Eventually, on increasing sample temperature, the width of β -MnAs stripes increases and also H_{bias}^x starts to become effective. At this stage, Fe/ α -MnAs regions and Fe/ β -MnAs ones behave as two distinct magnetic domains. We must note that there is a slight discrepancy concerning the exact value at which evidence of two distinct Fe phases is provided: in

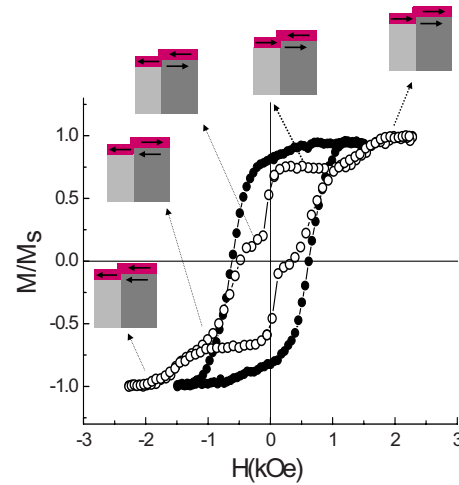


FIG. 7. (Color online) MOKE loops of the MnAs/GaAs(001) template (full symbols) and of the Fe/MnAs/GaAs(001) system (open symbols), measured at sample temperatures $T=315$ K. Sketches of the magnetization configuration are reported in the insets.

the FMR spectra the two Fe modes appear at $T=304$ K whereas two distinct Fe magnetization reversals are visible only above $T=308$ – 310 K in the MOKE measurements. This slight discrepancy is probably due to the fact that the magnetization reversal mechanism of Fe/ β -MnAs is driven by that of the α -MnAs stripes up to $T=310$ K. It is only when the value of H_{bias}^x becomes smaller than the coercive field of MnAs, that the MOKE technique becomes sensitive to the existence of the Fe/ β -MnAs domains. In this regard, the FMR technique proved to be a more sensitive tool for detecting the incipient Fe/ β -MnAs domains.

Concerning the evolution of the FMR peaks, the resonance field of the peak associated with Fe/ α -MnAs regions increases with temperature (upper panel of Fig. 3) because the combined effect of H_{dem}^x and of the MnAs morphology makes the direction perpendicular to the stripes harder and harder for such domains. On the contrary, the resonance field of the peak associated with the Fe/ β -MnAs regions assumes small values because, for the latter magnetic domains, the direction perpendicular to the stripes is an easy axis owing to the effect of both the in-plane magnetic anisotropy and H_{bias}^x . On increasing temperature, the resonance field of this mode begins to increase since, as the β stripes gradually widen, the system tends to the behavior of the continuous film. Interestingly, in this temperature range the magnetization alignment of adjacent Fe regions switches from a parallel to an antiparallel configuration only changing the intensity of the external applied field. This behavior can be clearly observed in the hysteresis loop measured at 315 K, which is shown in Fig. 7 together with the magnetization configuration of the various domains at different stages of the reversal process. For positive saturation, the magnetizations of the two Fe regions are parallel to each other, and to the magnetization of α -MnAs stripes in the substrate. Upon decreasing the external field, the magnetization of the Fe/ α -MnAs stripes starts to rotate due to the effect of H_{dem}^x , until an antiparallel alignment is realized with the magnetization of both the underlying

α -MnAs stripes and of the adjacent Fe/ β -MnAs stripes (the latter remain aligned with the external field). Around zero field, also the Fe/ β -MnAs stripes switch their magnetization, through an irreversible jump, and a parallel alignment of the two families of Fe domains is recovered again. On further reducing the magnetic field, one can observe (at about -600 Oe) the MnAs reversal, which in turn induces a new reversal of Fe/ α -MnAs via H_{dem} . The negative saturation of the whole system is reached through a coherent rotation of Fe/ α -MnAs.

Finally, let us briefly discuss the Fe behavior when the magnetic field is applied along the direction parallel to the stripes [lower panel of Fig. 3]. Since in the FMR experiments, the Fe magnetization is parallel to the external magnetic field, it is clear from Eq. (4) that in such a configuration the action of both H_{bias} and H_{dem} is null. Therefore, in the whole temperature range we observed only a single peak, whose temperature evolution is affected only by the shape anisotropy induced by the striped morphology. For sample temperature lower than about 300 K, the resonance field H_r^{Fe} decreases with increasing temperature since the effect of the substrate morphology makes the direction parallel to the stripes more favorable for both Fe/ α -MnAs and β -MnAs regions. In contrast, for sample temperature higher than about 304 K, the FMR behavior is dominated by the Fe/ β -MnAs stripes: H_r^{Fe} grows with increasing temperature because the β -MnAs stripes become wider and wider, until the system eventually recovers the behavior of the continuous film.

As a conclusive remark, it has to be noted that the effect of the MnAs transition on the resonance field of Fe is much more pronounced along the easy direction than along the hard one. This indicates that the stray fields are the main responsible of the Fe behavior during the coexistence of the two magnetic phases whereas the shape anisotropy of Fe stripes has a minor influence.

VI. CONCLUSIONS

The complex magnetic behavior of an ultrathin Fe film epitaxially grown onto MnAs/GaAs(001) has been investigated by means of FMR and MOKE experiments. The MnAs substrate is characterized by a magnetostructural phase transition that leads to a self-organized stripe pattern in a finite temperature range. During the coexistence of the α and β MnAs stripes, the Fe film is strongly influenced by the dipolar (stray) fields arising from the substrate, showing the coexistence of two distinct families of striped Fe domains. The theoretical analysis of the FMR data of the Fe overlayer has been performed, in the whole investigated temperature range, using a free-energy density model which allows an accurate determination of temperature-dependent magnetic parameters (both anisotropy constants and stray fields). Furthermore, the hysteresis loops indicate that, at the beginning of the MnAs phase transition, the magnetization reversal occurs through a coherent rotation, leading to an antiparallel alignment between the magnetization of the Fe overlayer and that of the MnAs substrate. On the contrary, when the stripe pattern is well defined, the magnetization reversal of the Fe/ α -MnAs and Fe/ β -MnAs domains takes place through two different and independent mechanisms. This temperature evolution of the Fe magnetization curves has been explained taking into account the effect of the stray fields produced by the α -MnAs stripes.

ACKNOWLEDGMENTS

J.M. and G.A. are researchers of CONICET. J.M. acknowledges Mairie de Paris and, also, Italian CNR for financial support from Short Term Mobility Program 2008. Financial support by the Ministero per l'Università e la Ricerca under PRIN-2007 project (Prot. Grant No. 2007X3Y2Y2) is acknowledged. This work was also partially granted by ANPCyT under Grants No. PICT 25748 (2004) and No. PICT 32684 (2005).

*milano@cab.cnea.gov.ar

¹I. Žutić, J. Fabian, and S. Das Sarma, *Rev. Mod. Phys.* **76**, 323 (2004).

²L. Däweritz, *Rep. Prog. Phys.* **69**, 2581 (2006), and references therein.

³R. H. Wilson and J. S. Kasper, *Acta Crystallogr.* **17**, 95 (1964); C. P. Bean and D. S. Rodbell, *Phys. Rev.* **126**, 104 (1962).

⁴V. M. Kaganer, B. Jenichen, F. Schippan, W. Braun, L. Däweritz, and K. H. Ploog, *Phys. Rev. Lett.* **85**, 341 (2000).

⁵V. M. Kaganer, B. Jenichen, F. Schippan, W. Braun, L. Däweritz, and K. H. Ploog, *Phys. Rev. B* **66**, 045305 (2002).

⁶R. Engel-Herbert, T. Hesjedal, J. Mohanty, D. M. Schaadt, and K. H. Ploog, *Phys. Rev. B* **73**, 104441 (2006).

⁷V. Garcia, Y. Sidis, M. Marangolo, F. Vidal, M. Eddrief, P. Bourges, F. Maccherozzi, F. Ott, G. Panaccione, and V. H. Etgens, *Phys. Rev. Lett.* **99**, 117205 (2007).

⁸R. Breitwieser, F. Vidal, I. L. Graff, M. Marangolo, M. Eddrief, J.-C. Boulliard, and V. H. Etgens, *Phys. Rev. B* **80**, 045403

(2009).

⁹B. Rache Salles, F. Vidal, V. H. Etgens, R. Breitwieser, M. Marangolo, and M. Eddrief, *Physica B* **404**, 2684 (2009).

¹⁰R. Breitwieser, M. Marangolo, J. Lüning, N. Jaouen, L. Joly, M. Eddrief, V. H. Etgens, and M. Sacchi, *Appl. Phys. Lett.* **93**, 122508 (2008).

¹¹M. Sacchi, M. Marangolo, C. Spezzani, L. Coelho, R. Breitwieser, J. Milano, and V. H. Etgens, *Phys. Rev. B* **77**, 165317 (2008).

¹²M. Sacchi, M. Marangolo, C. Spezzani, R. Breitwieser, H. Popescu, R. Dealounay, B. Rache Salles, M. Eddrief, and V. H. Etgens, *Phys. Rev. B* **81**, 220401 (2010).

¹³S. Tacchi, M. Madami, G. Carlotti, G. Gubbiotti, M. Marangolo, J. Milano, R. Breitwieser, V. H. Etgens, R. L. Stamps, and M. G. Pini, *Phys. Rev. B* **80**, 155427 (2009).

¹⁴G. Alejandro, L. B. Steren, J. Milano, A. Butera, M. Eddrief, and V. H. Etgens, *J. Magn. Magn. Mater.* **320**, e408 (2008).

¹⁵M. Tanaka, J. P. Harbison, M. C. Park, T. Shin, and G. M. Roth-

- berg, *Appl. Phys. Lett.* **65**, 1964 (1994).
- ¹⁶*Ultrathin Magnetic Structures*, edited by B. Heinrich and J. A. C. Bland (Springer, Berlin, 1994), Vol. II.
- ¹⁷Values of the resonance field H_r^{Fe} greater than 2.1 kG could not be measured for temperatures higher than 310 K because the resonance modes become too wide for calculating rigorously the resonance fields.
- ¹⁸M. Grimsditch, S. Kumar, and E. E. Fullerton, *Phys. Rev. B* **54**, 3385 (1996).
- ¹⁹J. Smit and H. G. Beljers, *Philips Res. Rep.* **10**, 113 (1955).
- ²⁰M. Farle, *Rep. Prog. Phys.* **61**, 755 (1998); M. Farle, A. N. Anisimov, W. Platow, P. Pouloupoulos, and K. Baberschke, *J. Magn. Magn. Mater.* **198-199**, 325 (1999).
- ²¹C. A. F. Vaz, J. A. C. Bland, and G. Lauhoff, *Rep. Prog. Phys.* **71**, 056501 (2008), and references therein.
- ²²F. Bensch, R. Moosbüler, and G. Bayreuther, *J. Appl. Phys.* **91**, 8754 (2002).
- ²³H. B. Callen and E. Callen, *J. Phys. Chem. Solids* **27**, 1271 (1966).
- ²⁴B. D. Cullity, *Introduction to Magnetic Materials* (Addison-Wesley, Reading, MA, 1972).
- ²⁵In fact, in Ref. 13 the fitted values of the effective out-of-plane anisotropy field, in-plane uniaxial field, and cubic anisotropy field were $H_{\perp}=6.5$ kG, $H_{\parallel}=0.16$ kG, and $H_K=0.15$ kG, to be compared, respectively, with the values 6.1, 0.160, and 0.123 kG, obtained from Fig. 4 at $T=325$ K.
- ²⁶L. B. Steren, J. Milano, V. Garcia, M. Marangolo, M. Eddrief, and V. H. Etgens, *Phys. Rev. B* **74**, 144402 (2006).
- ²⁷The reason for this approximation is twofold: (i) the irregular shape of the stripes prevents a quantitative evaluation of the shape anisotropy of Fe domains versus temperature; (ii) owing to the reduced thickness of the Fe overlayer, the effective fields associated with the shape anisotropy of the Fe stripes are expected to be smaller than the stray fields produced by the striped MnAs substrate.
- ²⁸L. N. Coelho, B. R. A. Neves, R. Magalhães-Paniago, F. C. Vicentin, H. Westfahl, Jr., R. M. Fernandes, F. Iikawa, L. Däw-eritz, C. Spezzani, and M. Sacchi, *J. Appl. Phys.* **100**, 083906 (2006).